LETTER

doi:10.1038/nature10421

Interannual variability in the oxygen isotopes of atmospheric CO_2 driven by El Niño

Lisa R. Welp[1], Ralph F. Keeling[1], Harro A. J. Meijer[2], Alane F. Bollenbacher[1], Stephen C. Piper[1], Kei Yoshimura[1]†, Roger J. Francey[3], Colin E. Allison[3] & Martin Wahlen[1]

The stable isotope ratios of atmospheric CO_2 ($^{18}O/^{16}O$ and $^{13}C/^{12}C$) have been monitored since 1977 to improve our understanding of the global carbon cycle, because biosphere–atmosphere exchange fluxes affect the different atomic masses in a measurable way[1]. Interpreting the $^{18}O/^{16}O$ variability has proved difficult, however, because oxygen isotopes in CO_2 are influenced by both the carbon cycle and the water cycle[2]. Previous attention focused on the decreasing $^{18}O/^{16}O$ ratio in the 1990s, observed by the global Cooperative Air Sampling Network of the US National Oceanic and Atmospheric Administration Earth System Research Laboratory. This decrease was attributed variously to a number of processes including an increase in Northern Hemisphere soil respiration[3]; a global increase in C_4 crops at the expense of C_3 forests[4]; and environmental conditions, such as atmospheric turbulence[5] and solar radiation[6], that affect CO_2 exchange between leaves and the atmosphere. Here we present 30 years' worth of data on $^{18}O/^{16}O$ in CO_2 from the Scripps Institution of Oceanography global flask network and show that the interannual variability is strongly related to the El Niño/Southern Oscillation. We suggest that the redistribution of moisture and rainfall in the tropics during an El Niño increases the $^{18}O/^{16}O$ ratio of precipitation and plant water, and that this signal is then passed on to atmospheric CO_2 by biosphere–atmosphere gas exchange. We show how the decay time of the El Niño anomaly in this data set can be useful in constraining global gross primary production. Our analysis shows a rapid recovery from El Niño events, implying a shorter cycling time of CO_2 with respect to the terrestrial biosphere and oceans than previously estimated. Our analysis suggests that current estimates of global gross primary production, of 120 petagrams of carbon per year[7], may be too low, and that a best guess of 150–175 petagrams of carbon per year better reflects the observed rapid cycling of CO_2. Although still tentative, such a revision would present a new benchmark by which to evaluate global biospheric carbon cycling models.

Quantifying global-scale gross primary production (GPP) has been difficult because there are no direct measures at scales greater than the leaf level. Consequently, inferences are made from atmospheric-based CO_2 flux measurements (for example eddy covariance[7]), but these can only measure the net ecosystem exchange, that is, the small residual between GPP and ecosystem respiration. Satellite-based observations estimate GPP on the basis of absorbed photosynthetic radiation[8]. Both approaches rely heavily on biospheric process models to generate GPP estimates. We present a new approach that does not depend on biospheric process models, using existing long-term time series of CO_2 isotopes to quantify mean global GPP over the past several decades.

Stable isotope analysis of CO_2 started with flask samples from the South Pole (SPO) and Christmas Island stations in 1977 and later expanded to include the Alert (ALT), Point Barrow, La Jolla, Mauna Loa (MLO), Cape Kumukahi, American Samoa, Kermadec Islands and Baring Head stations. Figure 1 shows deseasonalized monthly mean $^{18}O/^{16}O$ observations and spline fits at each station expressed using delta notation, $\delta^{18}O = (^{18}O/^{16}O)_{sample}/(^{18}O/^{16}O)_{VPDB} - 1$, with the Vienna Pee Dee Belemnite (VPDB) standard. Interannual variability of $\delta^{18}O$-CO_2 (that is, $\delta^{18}O$ of the CO_2 samples) is characterized by oscillations of 2–10 yr, with relatively consistent timing and magnitude of anomalies at all stations and without any persistent long-term trend. The lack of a trend in $^{18}O/^{16}O$ contrasts with the increasing trend in the CO_2 mixing ratio, of roughly 1.5 p.p.m. yr^{-1}, and the decreasing trend in $\delta^{13}C = (^{13}C/^{12}C)_{sample}/(^{13}C/^{12}C)_{VPDB} - 1$, of -0.02‰ yr^{-1}, over the same period[1]. This is consistent with the fact that fossil fuel emissions contribute little to the $^{18}O/^{16}O$ budget of CO_2, and that oxygen atoms in CO_2 are renewed by exchange with oxygen atoms of water in leaves, soils and sea water approximately every 2 yr (refs 2, 9, 10) or less, as will be discussed below. Fortunately, signal-to-noise ratios are generally much larger for $\delta^{18}O$ than for $\delta^{13}C$ in CO_2.

Cross-correlation analysis determined that $\delta^{18}O$-CO_2 anomalies at station SPO lag anomalies at the low-latitude station MLO by 4–5 months. Stations ALT and PTB, which are at high northern latitudes, lag MLO by 3–4 months. This suggests that anomalies start in the tropics and propagate to high latitudes over the course of several months. Maximum correlation coefficients between SPO and both MLO and ALT were approximately 0.4 when allowing for lags between stations.

During El Niño/Southern Oscillation (ENSO) events, there are significant changes in the amount and intensity of rainfall in the tropics, especially over Southeast Asia and northern South America[11]. Changes in the amount of precipitation also affect the $\delta^{18}O$ value of water through the 'amount effect' and related processes[12]. Figure 2 shows the correlation between the ENSO precipitation index[13] (ESPI) and the $\delta^{18}O$ value of precipitation as hindcast by the IsoGSM model[14] driven by reanalysis winds. During El Niño years, the $\delta^{18}O$ value of precipitation (δ_{ppt}) increases in regions where the amount of precipitation decreases, such as Southeast Asia and northern South America. These are also regions with very high annual net primary production (NPP) and GPP. Figure 3a, b shows that $\delta^{18}O$-CO_2 is strongly positively correlated with δ_{ppt} in the tropics, whereas Fig. 3c, d shows that in the same regions it is negatively correlated with relative humidity. This further supports a link between $\delta^{18}O$-CO_2 and ENSO variability through the tropical water cycle.

The interannual variability of $\delta^{18}O$-CO_2 measured by the Scripps Institution of Oceanography (SIO) flask network was confirmed by comparison with an independent record of similar length from Cape Grim (CGO) station as measured by the Commonwealth Scientific and Industrial Research Organisation[15] (CSIRO), also shown in Fig. 1. CGO and SPO have very similar correlations with ENSO forcing, lagging ENSO by 8–11 months with maximum correlation coefficients of 0.4. SIO flask observations were also compared with those of the US National Oceanic and Atmospheric Administration Earth System Research Laboratory (Supplementary Information, section 1).

[1]Scripps Institution of Oceanography, University of California San Diego, 9500 Gilman Drive, La Jolla, California 92093-0244, USA. [2]Center for Isotope Research, University of Groningen, Nijenborgh 4, 9747 AG Groningen, The Netherlands. [3]CSIRO Marine and Atmospheric Research, PB 1, Aspendale, Victoria 3195, Australia. †Present address: Atmosphere and Ocean Research Institute, University of Tokyo, 5-1-5 Kashiwanoha, Kashiwa, Chiba 277-8568, Japan.

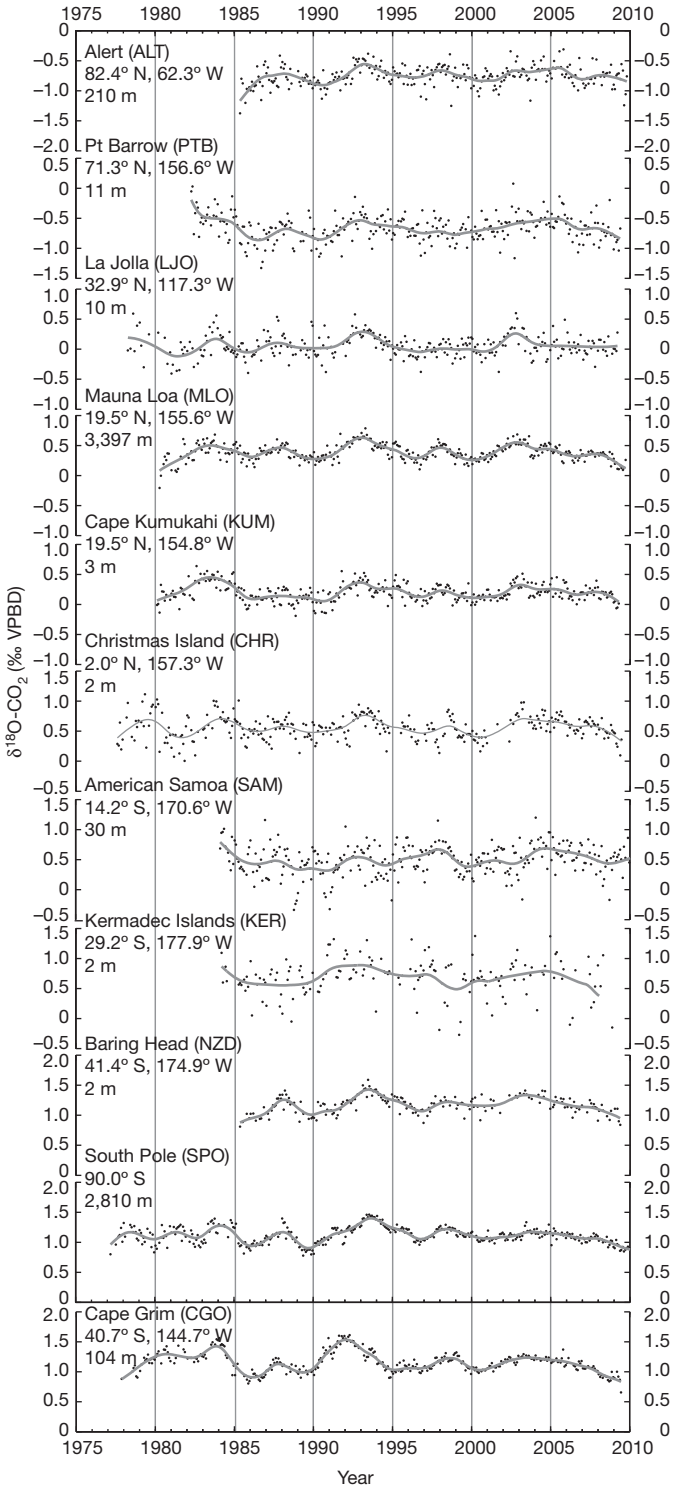

Figure 1 | Measurements of δ^{18}O-CO_2 from the SIO flask network and CSIRO. Monthly mean deseasonalized δ^{18}O-CO_2 station data (black dots) with long-term spline fits (grey lines). All stations (latitude, longitude and altitude as shown) are from the SIO flask network with the exception of the CSIRO station CGO, at the bottom of the figure. A seasonal harmonic fit was subtracted from the monthly means to produce the deseasonalized observations presented here. The 1σ mass spectrometer precision of both laboratories since 1990 is ~0.014‰. The SIO estimates that the 1σ error of duplicate flask measurements is ~0.025‰. Measurement uncertainties for both laboratories are larger before 1990.

We used a simple empirical model to demonstrate that the interannual variability in δ^{18}O-CO_2 is closely related to a low-pass filter of ENSO. The model follows from mass balance considerations (see

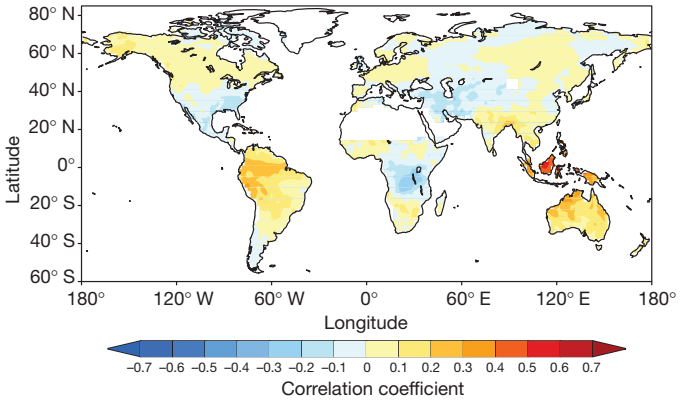

Figure 2 | Correlations between precipitation δ^{18}O from IsoGSM and ENSO. We use the ENSO precipitation index (ESPI) as a proxy for ENSO variability. Positive correlation indicates that precipitation is enriched in ^{18}O during the El Niño phase.

Supplementary Information, section 2, for a full derivation), treating the troposphere as two well-mixed boxes, one for the Northern Hemisphere and one for the Southern Hemisphere (N and S, respectively), assuming a linear ENSO forcing on the δ^{18}O-CO_2 values for each hemisphere (δ_N and δ_S, respectively) through the influence of the terrestrial biosphere and incorporating non-ENSO background processes that effectively damp the ENSO isotope anomalies:

$$\frac{d\delta_N'}{dt} = f_N \times A \times \mathrm{ENSO}'(t-\mathrm{lag}) - \frac{\delta_N'}{\tau_N} + \frac{\delta_S' - \delta_N'}{\tau_{mix}} \quad (1)$$

$$\frac{d\delta_S'}{dt} = (1-f_N) \times A \times \mathrm{ENSO}'(t-\mathrm{lag}) - \frac{\delta_S'}{\tau_S} + \frac{\delta_N' - \delta_S'}{\tau_{mix}} \quad (2)$$

Fitting parameters include f_N, A, τ_N, τ_S and lag, where f_N represents the fraction of the total ENSO forcing within the Northern Hemisphere; A is the scaling term in units of ‰ $\mathrm{ESPI}^{-1}\,\mathrm{yr}^{-1}$, and represents the conversion of the ESPI anomalies from the mean (ENSO′) into δ^{18}O-CO_2 anomalies from the mean (δ_N' or δ_S', depending on hemisphere); τ_N and τ_S are the Northern Hemisphere and Southern

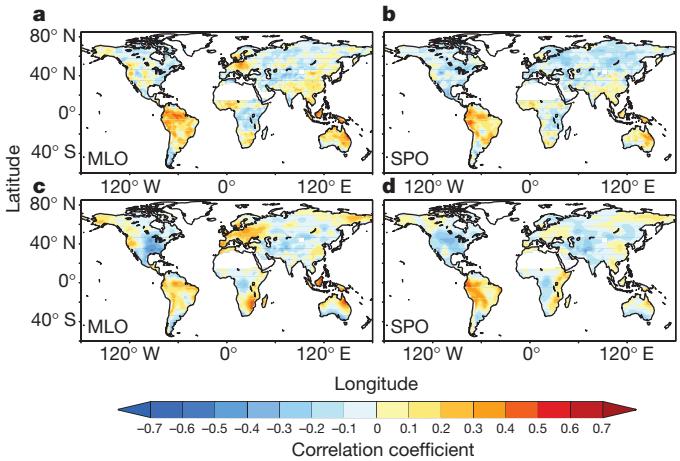

Figure 3 | Correlations between flask δ^{18}O-CO_2 records and precipitation δ^{18}O and relative humidity from IsoGSM. **a**, **b**, Correlation between the previous 9-month running mean of precipitation δ^{18}O and the monthly mean deseasonalized δ^{18}O-CO_2 from station MLO (**a**) and station SPO (**b**). Positive correlations indicate that δ^{18}O-CO_2 increases when precipitation δ^{18}O increases. **c**, **d**, Correlation between the NPP-weighted, 9-month running mean of negative relative humidity and deseasonalized δ^{18}O-CO_2 from MLO (**c**) and SPO (**d**). Positive correlations indicate that δ^{18}O-CO_2 increases when relative humidity decreases. NPP-weighted relative humidity was used here to give weight to months with higher vegetation productivity when leaf-water isotope anomalies are passed onto CO_2.

Hemisphere turnover times of oxygen atoms in CO_2; and lag is the temporal offset between ESPI and the isotopic ENSO forcing. The constant τ_{mix}, which represents the interhemispheric mixing time, was set to a value of 12 months.

The box model approach assumes that surface $\delta^{18}O$-CO_2 measurements represent the entire tropospheric column. Although aircraft measurements have observed variability within the troposphere, the fact that the seasonal cycle of $\delta^{18}O$-CO_2 observed at MLO is similar to that in the upper troposphere[16] means that the box model may be a sufficient first attempt because we are tracking a signal that originates in the tropics and is transported vertically before reaching the mid latitudes.

We alternately used MLO and ALT to represent the Northern Hemisphere box, and SPO and CGO for the Southern Hemisphere box (Supplementary Information, section 3). We repeated the fits using 1,000 hypothetical time series with the same autocorrelation as the ENSO index but with random phase[17]. All station combinations gave fits to the true ENSO index that were better than a large majority of fits using the hypothetical indices, more than 98% of cases using the SIO station combinations and more than 93% using SIO–CSIRO station combinations (Supplementary Information, section 4). The MLO–SPO combination of data from 1980 to 2009 yielded the best fit between the ENSO model and observations (Fig. 4).

The model fit yielded a short turnover time of $\tau_N = 0.4$–0.8 yr for $\delta^{18}O$-CO_2 in the Northern Hemisphere, depending on the stations used in the analysis and with 1σ errors not greater than 0.3 yr. Sensitivity analysis of the model parameter fit covariance suggested that τ_S is greater than 2 yr, but the upper bound was difficult to determine because of the 1-yr interhemispheric mixing time (τ_{mix}). We expected τ_N to be less than τ_S given the larger land biosphere and the greater exchange of CO_2 with leaf and soil water in the north. Estimated turnover times for the two hemispheres based on gross exchanges with the ocean[18] and the terrestrial biosphere[19] indicated that the Southern Hemisphere turnover time is ~120% longer than that of the Northern Hemisphere. The model-derived, hemisphere-specific turnover times correspond to a global tropospheric mean of 0.7–1.4 yr. Allowing for the 22% of the atmospheric mass contained in the stratosphere[20], which was not included in the model, the estimated global atmospheric turnover time increases to 0.9–1.7 yr.

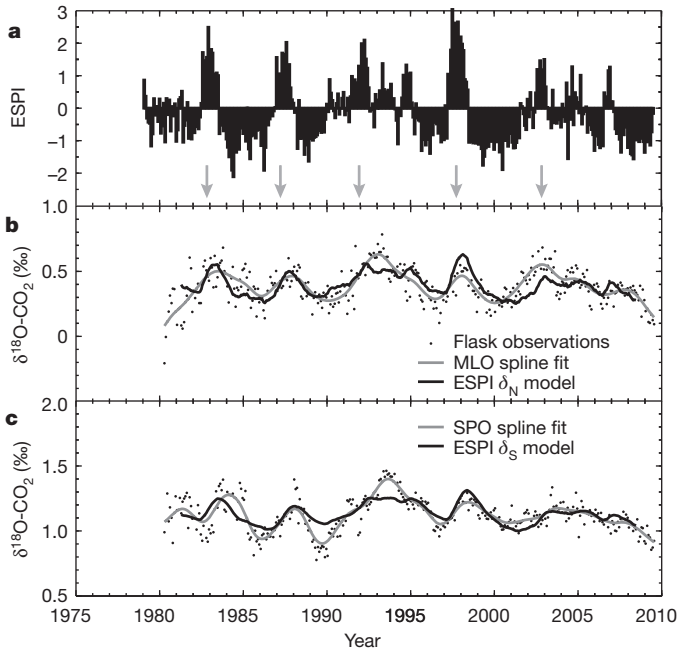

Figure 4 | ENSO index and two-box model results. **a**, ESPI was used as a proxy for ENSO variability. Arrows denote El Niño events. **b**, Empirical ENSO model fit for the Northern Hemisphere (δ_N, black line), compared with the deseasonalized monthly flask observations (black dots) and spline fit or interannual variability at station MLO (grey line). **c**, Same as in **b** but for the Southern Hemisphere model fit (δ_S) and station SPO.

These atmospheric observations suggest that the turnover time for oxygen atoms in CO_2 may be slightly lower than previously published estimates. Turnover times of oxygen in CO_2 of 1.7 yr (ref. 2) and 1.5 yr (ref. 10) have been estimated from bottom-up flux estimates using process models. These estimates are sensitive to assumed values for GPP and the ratio of CO_2 concentration inside the leaf relative to the atmosphere. Our turnover time estimate using $\delta^{18}O$-CO_2 anomalies is independent of these assumptions. Recent efforts to balance the carbonyl sulphide budget also point to more exchange of CO_2 between the atmosphere and land vegetation than previously estimated[21]. Field studies have indicated that carbonic anhydrase in soils catalyses the direct exchange of oxygen isotopes between soil water and CO_2. A recent global estimate of this soil equilibration flux could bring the global turnover time of ref. 10 down as low as ~0.9 yr (ref. 22).

The parameter A provides insight into the mechanisms linking $\delta^{18}O$-CO_2 to ENSO climate anomalies. The fits yielded A values of 0.27 to 0.35‰ $ESPI^{-1}\,yr^{-1}$, depending on the stations used, with 1σ errors of less than 0.08‰ $ESPI^{-1}\,yr^{-1}$. To assess which processes contribute most to A, we carried out a scale analysis of the mass balance of ^{18}O in CO_2 (Supplementary Information, section 5). We identified two dominant processes. The first was a change in the δ_{ppt} value associated with ENSO events. Precipitation $\delta^{18}O$ anomalies are directly transmitted to soil and leaf water, and hence contribute to the $\delta^{18}O$ value of CO_2. Generally, the δ_{ppt} value on land in the tropics increases during El Niño events, as evidenced by isotopic studies of precipitation[23,24], tropical ice cores[25], tree rings[26] and isotope-enabled general circulation models[14]. The second dominant effect was an increase in the isotopic enrichment of leaf water relative to soil water caused by lower relative humidity during warm and dry El Niño events in the tropics than in La Niña years[27].

We estimate that the effects of δ_{ppt} and relative humidity are similar in magnitude and reinforce each other. The magnitude of A can be accounted for if we assume that anomalies in δ_{ppt} and relative humidity influenced 40% of the global land CO_2 fluxes. NPP from 20° S to 20° N is about 40% of global NPP[19], lending support that the global anomalies of $\delta^{18}O$ in CO_2 may be generated by the tropical land biosphere that is modulated by ENSO. Our analysis showed that many other possible processes were less important, including changes in CO_2 fluxes (for example those related to drought) and fire emissions. Our analysis neglected ENSO-related changes in air–sea CO_2 exchange, in stratosphere–troposphere exchange and in diffuse light, which are also likely to be small.

The model-derived fraction of isotopic ENSO forcing injected into the Northern Hemisphere (f_N) was 0.49–0.76 depending on the station combinations used. Lags between ESPI and atmospheric $\delta^{18}O$-CO_2 forcing were small, ranging from −2 months to 1 month, and had 1σ errors of 1 month. The model thus successfully accounts for the observed lag between ESPI and $\delta^{18}O$-CO_2 through the finite hemispheric turnover times.

We can relate our model-derived turnover time to the gross flux of CO_2 equilibrating with the ocean and land surface water. This gross exchange flux can be used to estimate GPP by subtracting air–sea exchange; the amount of CO_2 that escapes leaf interiors without being fixed into organic matter, which is directly related to the ratio of CO_2 inside the leaf to that in the atmosphere; and the soil invasion flux (Supplementary Information, section 6). Reconciling the short turnover time (0.9–1.7 yr) with current understanding of the global carbon budget would require that the soil invasion CO_2 flux be near the upper case considered in ref. 22 and much greater than soil respiration. At present, there are not enough field observations to confirm such high fluxes of soil invasion. Alternatively, and more plausibly, the fast response can be accounted for by revising global GPP upwards from 120 Pg C yr^{-1} (ref. 7) to 150–175 Pg C yr^{-1}. Using this approach, we

argue that 120 Pg C yr^{-1} may actually be a lower bound on GPP. (See Supplementary Information, section 6, for more discussion.)

The timescale of the damping of the ENSO $\delta^{18}O$-CO_2 signal provides a constraint on global GPP without the need for detailed isotopic modelling of multiple surface water pools. We have achieved with $\delta^{18}O$-CO_2 what was believed to be possible only by combining ^{17}O and ^{18}O data from CO_2 (ref. 28). These results can be used to validate biospheric components of carbon cycle models used to predict future climate change. The measurements and modelling presented here highlight the significance of $\delta^{18}O$-CO_2 long-term records as integrators of the carbon and water cycles.

METHODS SUMMARY

Air samples were collected, without drying, in evacuated 5-l glass flasks with a single glass stopcock lubricated with Apiezon grease, and were returned to the laboratory for analysis. Until 1992, isotopic analysis was performed at the CIO University of Groningen, The Netherlands; since then, it has been done at the SIO, La Jolla, California. Offsets between the laboratories have been investigated and corrected[29]. We curve fitted the daily mean of replicate flask samples with spline and seasonal harmonic components, and monthly means were constructed from observations adjusted to the fifteenth day of each month[30]. The interannual variability is simply the spline component of the curve fit. Deseasonalized monthly means were calculated by subtracting the seasonal harmonic component from the monthly mean observations.

Parameter fitting of the two-box model was done using a nonlinear least-squares data fitting function in MATLAB ('lsqnonlin') to find the minimum of the sum of squares of the differences between deseasonalized monthly mean flask observations from one station in each hemisphere and the model predictions from equations (1) and (2), weighted by $1/\sigma$ for each station. Estimates of the 1σ error for each station's measurements were not obtained from the mass spectrometer precision but rather from the standard deviation of the residuals between the deseasonalized monthly mean flask observations and the spline fits, which were ~0.08‰.

Isotope data of CO_2 from the SIO network is publicly available at http://scrippsco2.ucsd.edu/data/atmospheric_co2.html.

Received 22 July 2010; accepted 4 August 2011.

1. Keeling, C. D. *et al.* in *A History of Atmospheric CO_2 and Its Effects on Plants, Animals, and Ecosystems* (eds Ehleringer, J. R., Cerling, T. E. & Dearing, M. D.) 83–113 (Springer, 2005).
2. Farquhar, G. D. *et al.* Vegetation effects on the isotope composition of oxygen in atmospheric CO_2. *Nature* **363,** 439–443 (1993).
3. Ishizawa, M., Nakazawa, T. & Higuchi, K. A multi-box model study of the role of the biospheric metabolism in the recent decline of $\delta^{18}O$ in atmospheric CO_2. *Tellus B* **54,** 307–324 (2002).
4. Gillon, J. & Yakir, D. Influence of carbonic anhydrase activity in terrestrial vegetation on the ^{18}O content of atmospheric CO_2. *Science* **291,** 2584–2587 (2001).
5. Lee, X. H. *et al.* Canopy-scale kinetic fractionation of atmospheric carbon dioxide and water vapor isotopes. *Glob. Biogeochem. Cycles* **23,** GB1002 (2009).
6. Still, C. J. *et al.* Influence of clouds and diffuse radiation on ecosystem-atmosphere CO_2 and $CO^{18}O$ exchanges. *J. Geophys. Res.* **114,** G01018 (2009).
7. Beer, C. *et al.* Terrestrial gross carbon dioxide uptake: global distribution and covariation with climate. *Science* **329,** 834–838 (2010).
8. Zhao, M. S., Heinsch, F. A., Nemani, R. R. & Running, S. W. Improvements of the MODIS terrestrial gross and net primary production global data set. *Remote Sens. Environ.* **95,** 164–176 (2005).
9. Ciais, P. *et al.* A three-dimensional synthesis study of $\delta^{18}O$ in atmospheric CO_2. 1. Surface fluxes. *J. Geophys. Res.* **102,** 5857–5872 (1997).
10. Cuntz, M., Ciais, P., Hoffmann, G. & Knorr, W. A comprehensive global three-dimensional model of $\delta^{18}O$ in atmospheric CO_2: 1. Validation of surface processes. *J. Geophys. Res.* **108,** 4527 (2003).
11. Dai, A. & Wigley, T. M. L. Global patterns of ENSO-induced precipitation. *Geophys. Res. Lett.* **27,** 1283–1286 (2000).
12. Gat, J. R., Mook, W. G. & Meijer, H. A. J. *Environmental Isotopes in the Hydrological Cycle, Volume II: Atmospheric Water* 55, 56 (UNESCO/IAEA, 2001).
13. Curtis, S. & Adler, R. ENSO indices based on patterns of satellite-derived precipitation. *J. Clim.* **13,** 2786–2793 (2000).
14. Yoshimura, K., Kanamitsu, M., Noone, D. & Oki, T. Historical isotope simulation using reanalysis atmospheric data. *J. Geophys. Res.* **113,** D19108 (2008).
15. Allison, C. E. & Francey, R. J. Verifying Southern Hemisphere trends in atmospheric carbon dioxide stable isotopes. *J. Geophys. Res.* **112,** D21304 (2007).
16. Assonov, S. S., Brenninkmeijer, C. A. M., Schuck, T. J. & Taylor, P. Analysis of ^{13}C and ^{18}O isotope data of CO_2 in CARIBIC aircraft samples as tracers of upper troposphere/lower stratosphere mixing and the global carbon cycle. *Atmos. Chem. Phys.* **10,** 8575–8599 (2010).
17. Ebisuzaki, W. A method to estimate the statistical significance of a correlation when the data are serially correlated. *J. Clim.* **10,** 2147–2153 (1997).
18. Takahashi, T. S. *et al.* Climatological mean and decadal changes in surface ocean pCO_2, and net sea-air CO_2 flux over the global oceans. *Deep-Sea Res. II* **56,** 554–577 (2009).
19. Randerson, J. T., Thompson, M. V., Conway, T. J., Fung, I. Y. & Field, C. B. The contribution of terrestrial sources and sinks to trends in the seasonal cycle of atmospheric carbon dioxide. *Glob. Biogeochem. Cycles* **11,** 535–560 (1997).
20. Appenzeller, C., Holton, J. R. & Rosenlof, K. H. Seasonal variation of mass transport across the tropopause. *J. Geophys. Res.* **101,** 15071–15078 (1996).
21. Montzka, S. A. *et al.* On the global distribution, seasonality, and budget of atmospheric carbonyl sulfide (COS) and some similarities to CO_2. *J. Geophys. Res.* **112,** D09302 (2007).
22. Wingate, L. *et al.* The impact of soil microorganisms on the global budget of $\delta^{18}O$ in atmospheric CO_2. *Proc. Natl Acad. Sci. USA* **106,** 22411–22415 (2009).
23. Cobb, K. M., Adkins, J. F., Partin, J. W. & Clark, B. Regional-scale climate influences on temporal variations of rainwater and cave dripwater oxygen isotopes in northern Borneo. *Earth Planet. Sci. Lett.* **263,** 207–220 (2007).
24. Vuille, M. & Werner, M. Stable isotopes in precipitation recording South American summer monsoon and ENSO variability: observations and model results. *Clim. Dyn.* **25,** 401–413 (2005).
25. Thompson, L. G. Ice core evidence for climate change in the Tropics: implications for our future. *Quat. Sci. Rev.* **19,** 19–35 (2000).
26. Evans, M. N. Toward forward modeling for paleoclimatic proxy signal calibration: a case study with oxygen isotopic composition of tropical woods. *Geochem. Geophys. Geosyst.* **8,** Q07008 (2007).
27. Willett, K. M., Jones, P. D., Gillett, N. P. & Thorne, P. W. Recent changes in surface humidity: development of the HadCRUH dataset. *J. Clim.* **21,** 5364–5383 (2008).
28. Hoag, K. J., Still, C. J., Fung, I. Y. & Boering, K. A. Triple oxygen isotope composition of tropospheric carbon dioxide as a tracer of terrestrial gross carbon fluxes. *Geophys. Res. Lett.* **32,** L02802 (2005).
29. Bollenbacher, A. F. *et al. Calibration Methodology for the Scripps $^{13}C/^{12}C$ and $^{18}O/^{16}O$ Stable Isotope Program 1992–1996: a Report Prepared for the Global Environmental Monitoring Program of the World Meteorological Organization* (Scripps Institution of Oceanography, 2000).
30. Keeling, C. D. *et al. Exchanges of Atmospheric CO_2 and $^{13}CO_2$ with the Terrestrial Biosphere and Oceans from 1978 to 2000. I. Global Aspects*. SIO Reference No. 01–06 (Scripps Institution of Oceanography, 2001).

Supplementary Information is linked to the online version of the paper at www.nature.com/nature.

Acknowledgements The authors thank S. Walker for programming assistance and all those involved with flask collection and analysis. This work was supported by the US National Science Foundation (NSF) under grant ATM06-32770, by the US Department of Energy (DOE) under grant DE-SC0005099 and by the US National Aeronautics and Space Administration (NASA) under grant NNX11AF36G. Any opinions, findings and conclusions or recommendations expressed in this material are those of the authors and do not necessarily reflect the views of NSF, DOE or NASA.

Author Contributions L.R.W. analysed the data. R.F.K. supervised the project. L.R.W. and R.F.K. wrote the paper. H.A.J.M., A.F.B., R.J.F., C.E.A. and M.W. provided data. K.Y. provided the IsoGSM output. All authors discussed the results and commented on the manuscript.

Author Information Reprints and permissions information is available at www.nature.com/reprints. The authors declare no competing financial interests. Readers are welcome to comment on the online version of this article at www.nature.com/nature. Correspondence and requests for materials should be addressed to L.R.W. (lwelp@ucsd.edu) or R.F.K. (rkeeling@ucsd.edu).